Evolution of obliquity of a terrestrial planet due to gravitational perturbation by a giant planet

Keiko Atobe[1], Takashi Ito[2], and Shigeru Ida[1]

1. Departement of Earth and Planetary Sciences,

Tokyo Institute of Technology, Japan

2. Astronomical Data Analysis Computer Center,

National Astronomical Observatory, Japan

Abstract

We have studied the change in planetary obliquity near a spin-orbit resonance through numerical calculations and analytical arguments. To clarify basic process of the obliquity evolution, we have considered a simple system that consists of a host star, a hypothetical terrestrial planet, and a hypothetical giant planet. When the precession rate of the spin axis of the terrestrial planet coincides with the frequency of secular variations in its orbital inclination, spin-orbit resonance occurs and the obliquity of the terrestrial planet has large variations. We investigated time evolution of the obliquity near the resonance through numerical calculations of secular precession equations as well as analytical arguments. We derived the resonance width semi-analytically. Using this result, we predict the resonance region as a function of semi-major axis for a given giant planet.

1 Introduction

In general, the orientation of the planets' spin axis is not fixed, but changes all the time. Because of their equatorial bulge, planets are subject to torques arising from the gravitational forces of their satellites, host star and other planets. This causes precessional motion of the spin axis. Since the planets' orbits exhibit secular variations induced by gravitational perturbations exerted by other planets, the obliquity of the planets (the angle of the spin axis relative to the orbital plane) generally changes periodically, too. At present, Earth's spin has a precessional period of about 26,000 years, and its obliquity varies by $\pm$ 1.3 degrees around the mean value of 23.3 degree. Such obliquity variations would affect the planet's global climate through insolation change.

Ward (1974) and Ward & Rudy (1991) showed that large $\sim \pm 10$ degrees variations of the obliquity of Mars are caused by the spin-orbit resonance, employing the secular precession equations (Eq. (1)). Here, spin-orbit resonance means that the precession rate of the spin axis coincides with one of the eigenfrequencies of secular variations in the orbital inclination.

Overlapping of spin-orbit resonances may cause chaotic variations of the obliquity of terrestrial planets (Ward 1992, Laskar & Robutel 1993, Touma & Wisdom 1993). The maximum oscillation amplitude of orbital inclination at a spin-orbit resonance was approximately derived by Ward (1993), through a nonlinear analysis of the secular precession equations. If changes

in planetary orbital inclinations are quasi-periodic, secular perturbation theory (e.g., Brouwer & Clemence 1961) predicts locations of the spin-orbit resonances.

Laskar (1989) showed that orbital evolution of the terrestrial planets has Lyapunov time scale $\sim 10^7$ years, why may imply that the orbital evolution is chaotic on a timescale $\sim 10^7$ years (although their orbits are globally stable). The chaotic orbital evolution of planets results in more complicated obliquity changes (Laskar & Robutel 1993).

With Fourier spectrum of time-dependent eigenfrequencies for orbital inclination variations obtained by Laskar (1990), Laskar & Robutel (1993) integrated the secular precession equations with wide ranges of initial obliquity (ϵ_0) and the precession parameter (α). They found large chaotic regions in the ϵ_0-α plane and suggested that the obliquity of all the terrestrial planets except the Earth in the Solar system could have experienced large and chaotic variations.

Since the procedure to find the chaotic regions by Laskar & Robutel (1993) is rather complicated, it would not be easy to apply their results to more general extrasolar planetary systems. Laskar & Robutel (1993) suggested that arguments based on the spin-orbit resonances can be still used to understand qualitative features of their results. Here we are interested in obliquity variations of rocky planets in habitable zone in extrasolar planetary systems where a gas giant planet(s) has been detected. Large obliquity variations, even if they are not chaotic, may inhibit habitability.

For this purpose, we re-analyze the spin-orbit resonance in more general form. In order to clarify fundamental processes of obliquity evolution, we study a system containing a host star, a hypothetical terrestrial planet and a hypothetical giant planet, in wide parameter ranges. In particular, we investigate the behavior of obliquity near a resonance through analytical arguments and numerical calculations of the secular precession equations. In section 2, we briefly summarize the spin-orbit resonance. We show results of numerical calculations in section 3. In section 4, resonance width is derived semi-analytically. In section 5, we briefly discuss the regions for a hypothetical terrestrial planet where its obliquity variations become large by the spin-orbit resonance.

2 Basic Equations and Model

We consider a system containing a host star, a hypothetical terrestrial planet with axisymmetric shape and negligible mass, and a hypothetical giant planet. We assume the two planets initially have circular orbits around a host star. We numerically solve the orbit-averaged Euler equations (secular precession equations) given by Ward (1974):

$$\frac{d\hat{\boldsymbol{s}}}{dt} = \alpha(\hat{\boldsymbol{s}} \cdot \hat{\boldsymbol{n}})(\hat{\boldsymbol{s}} \times \hat{\boldsymbol{n}}), \tag{1}$$

where $\hat{\boldsymbol{s}}$ is a unit vector in the direction of the spin axis with components

$$s_x = \sin\theta \sin\psi, \tag{2}$$

$$s_y = -\sin\theta \cos\psi, \tag{3}$$

$$s_z = \cos\theta, \tag{4}$$

θ is the angle between the spin axis and the z-axis, and ψ is the longitude of the equator of the terrestrial planet in inertial frame. The precessional constant α is given by

$$\alpha = \frac{3G(C-A)}{2C\omega}\frac{M_1}{a^3}, \tag{5}$$

where G is the gravitational constant, M_1 is the mass of the host star. $(C-A)/C$, ω and a are the dynamical ellipticity, the spin rate, and the semi-major axis of the terrestrial planet, respectively. In our calculation, we assume $(C-A)/C$ and ω are constants.

$\hat{\boldsymbol{n}}$ is a unit vector normal to the orbital plane,

$$n_x = \sin I \sin \Omega, \tag{6}$$
$$n_y = -\sin I \cos \Omega, \tag{7}$$
$$n_z = \cos I, \tag{8}$$

where I is the orbital inclination and Ω is the longitude of the ascending node of the terrestrial planet. We here adopt the orbital plane of the giant planet as the reference frame. According to secular perturbation theories (e.g., Brouwer & Clemence 1961), the variations in I and Ω are given as

$$I = \text{const.}, \tag{9}$$
$$\Omega = -Bt + \Omega_0, \tag{10}$$

where Ω_0 is the initial ascending node of the terrestrial planet. B is

$$B = n \frac{1}{4} \frac{M_2}{M_1} {\alpha_2}^2 b_{3/2}^{(1)}(\alpha_2), \tag{11}$$

where n is the mean motion of the terrestrial planet, M_2 is the mass of the giant planet. α_2 is a/a_2, where a_2 is the semi-major axis of the giant planet. $b_{3/2}^{(1)}$ is a Laplace coefficient.

The obliquity of the terrestrial planet ϵ, the angle between $\hat{\boldsymbol{n}}$ and $\hat{\boldsymbol{s}}$, is obtained by

$$\hat{\boldsymbol{n}} \cdot \hat{\boldsymbol{s}} = \cos \epsilon. \tag{12}$$

The relationship between the reference plane, orbital plane and equator is schematically shown in Figure. 1.

Substitution of Eqs. (2) to (8) into (1) yields

$$\dot{\theta} \simeq \alpha \cos \epsilon \, I \, \sin(\psi - \Omega) + \mathcal{O}(I^2), \tag{13}$$
$$\dot{\psi} \simeq -\alpha \cos \epsilon + \mathcal{O}(I). \tag{14}$$

with the assumption $I \ll 1$ (Ward 1974; note that definition of ψ is different). We denote the precession frequency of the spin axis $\sim -\alpha \cos \epsilon$ by p_f. When $I \ll 1$, $\theta \simeq \epsilon$. Since the sign of $\dot{\theta}$ changes with frequency $(\dot{\psi} - \dot{\Omega})$, ϵ and θ usually oscillate with amplitude $\sim \mathcal{O}(I)$. However, when $\dot{\psi} - \dot{\Omega} \simeq -\alpha \cos \epsilon + B \simeq 0$, oscillation period of ϵ becomes very long and ϵ has a large amplitude. This is the spin-orbit resonance.

$\hat{\boldsymbol{n}}$ has dependence as $\hat{\boldsymbol{n}} = \hat{\boldsymbol{n}}(I, Bt)$. If we scale time by α^{-1}, Eq. (1) is transformed to

$$\frac{d\hat{\boldsymbol{s}}}{d\tilde{\tilde{t}}} = [\hat{\boldsymbol{s}} \cdot \hat{\boldsymbol{n}}(I, \frac{B}{\alpha}\tilde{\tilde{t}})][\hat{\boldsymbol{s}} \times \hat{\boldsymbol{n}}(I, \frac{B}{\alpha}\tilde{\tilde{t}})], \tag{15}$$

where $\tilde{\tilde{t}} = \alpha t$. This equation shows that the evolution path of $\hat{\boldsymbol{s}}$ is dependent only on the values of I and B/α. We will show that the evolution path near a resonance can be written as a form independent of I and B/α with further scaling of t and $\cos \epsilon$.

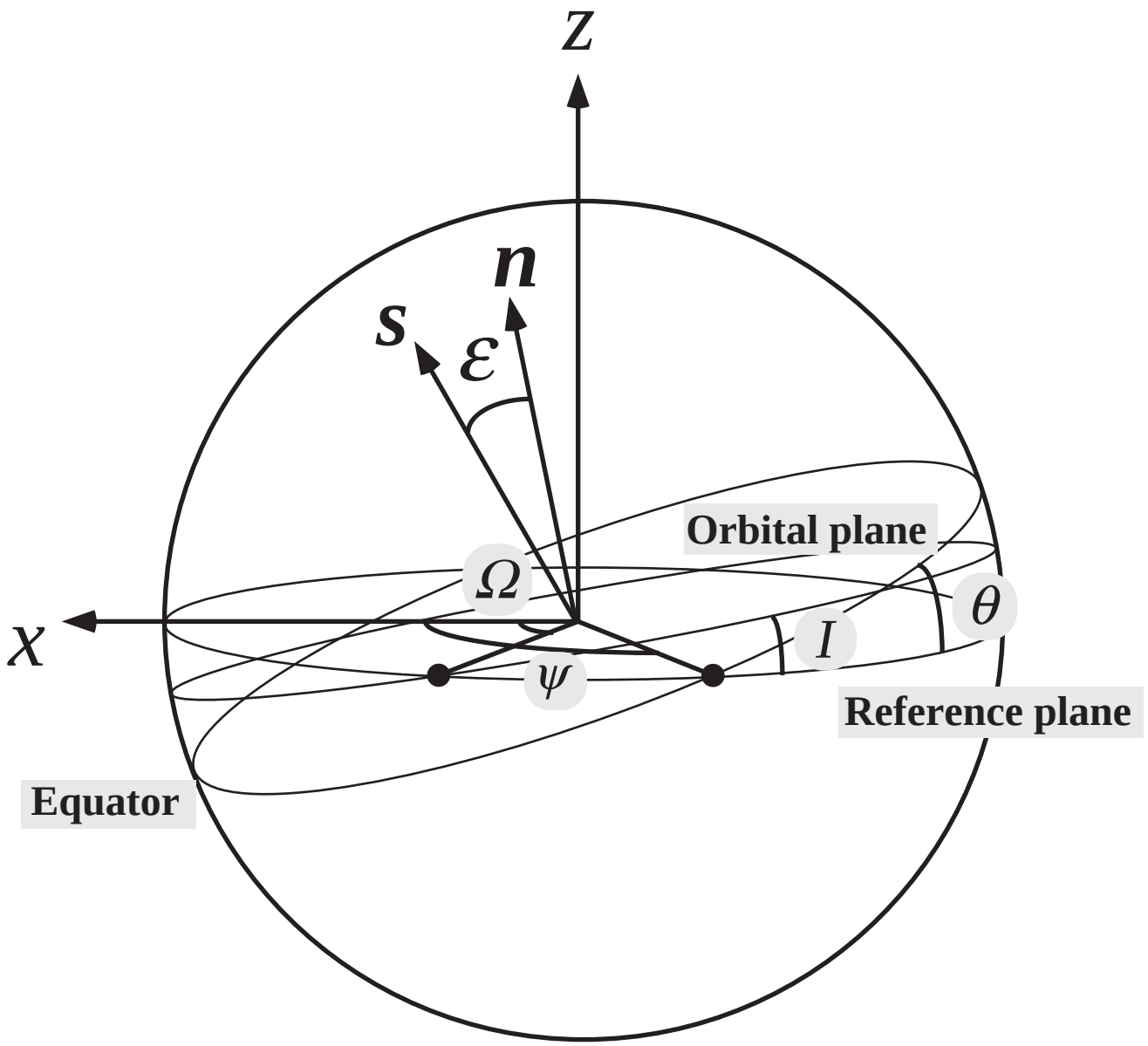

Figure 1: Relationship between the reference plane, orbital plane and equator. $\hat{\boldsymbol{s}}$ is the unit vector in the direction of the spin axis, $\hat{\boldsymbol{n}}$ is the unit vector normal to the orbital plane, ϵ is the obliquity, θ is the angle of the equator relative to the reference plane, ψ is the longitude of the equator, I is the orbital inclination, and Ω is the longitude of the ascending node.

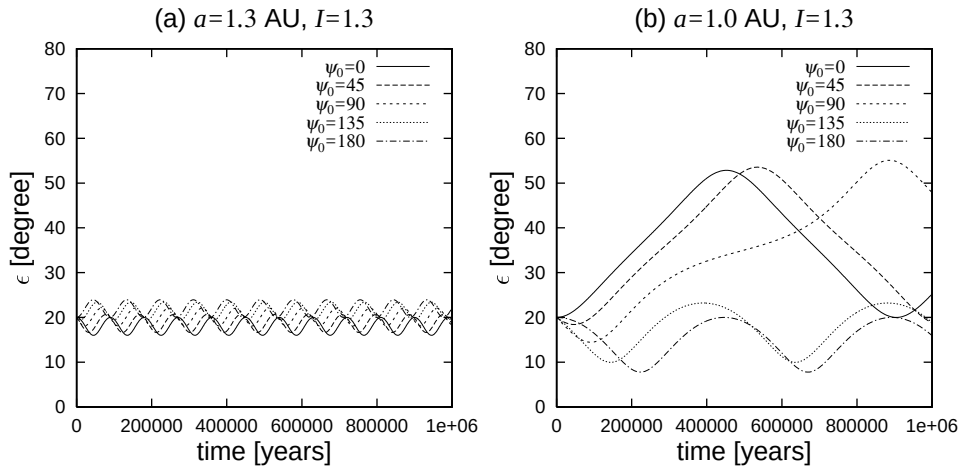

Figure 2: The time evolution of the obliquity ϵ of the terrestrial planet. ψ_0 is the initial longitude of the equator of the terrestrial planet, ψ.

3 Numerical Results

We integrate the precession equations (1) over 10^6 years, using a fourth order Runge-Kutta scheme. Here we adopt $(C-A)/A = 0.00335$, $\omega = 7.292 \times 10^{-5}$ rad/year, which are the same as the current Earth's values, $M_1 = M_\odot$, $a_2 = 5.2$ AU and $M_2 = 2M_J$ (M_J is the mass of Jupiter).

Figures 2 shows examples of time evolution of ϵ : (a) off-resonance case ($a = 1.3$ AU and $I = 1.3°$), (b) the case of resonance ($a = 1.0$ AU and $I = 1.3°$). Initial obliquity ϵ_0 is 20° in both cases. $\psi_0 - \Omega_0$, where ψ_0 is initial precession angle, is 0°, 45°, 90°, 135°, and 180°. ϵ oscillates regularly with periods $\sim 10^6$ years. In the off-resonance case, the variation amplitude is $\sim \mathcal{O}(I)$, while that in the resonance case is much larger than $\mathcal{O}(I)$.

To investigate the resonance width at $a = 1.0$ AU, we did similar calculations for different initial obliquity from 0° to 90° with 1° step size. The minimum and maximum values of ϵ plotted as a function of ϵ_0 in Figure 3 (the lower panel). p_f/α and B/α are also plotted in the upper panel. The resonance occurs when $p_f/\alpha \simeq B/\alpha$. Fig. 3 shows large resonance zone extending from 15° to 55° around exact resonant obliquity $\epsilon_* \simeq 40°$, where ϵ_* is defined by $B/\alpha = \cos\epsilon_*$. Even if it has the same initial obliquity, the amplitude depends on $\psi_0 - \Omega_0$.

To explain these features, we investigate evolution of $x \equiv \psi - \Omega$ and its time derivative $y \equiv (\dot{\psi} - \dot{\Omega})/\alpha\beta \simeq (-\alpha\cos\epsilon + B)/\alpha\beta$, where $\beta = \sqrt{I\cos\epsilon_*\sin\epsilon_*} = \sqrt{I(B/\alpha)\sqrt{1-(B/\alpha)^2}}$ (Eqs. (10) and (14)). The meaning of the scaling factor β for y will be clear later. Since α and B are fixed, the evolution of ϵ is uniquely determined by that of y. For $\psi_0 - \Omega_0 = \pi$, time evolution of y for the results in Fig. 3 is shown in Figure 4. Trajectories starts at $\psi_0 - \Omega_0 = \pi$ with different ϵ_0, that is different initial $y(= y_0)$. Trajectories with $-2 \lesssim y_0 \lesssim 2$ show libration around the center of $\alpha\cos\epsilon = B$ $(y = 0)$ and $\psi - \Omega = \pi$ $(x = \pi)$, while the other trajectories show

circulation. The former cases are "resonance". The trajectories with libration generally have large periodic variations, that is, large periodic obliquity variations. Note that as mentioned before, Eq. (1) is scaled with α and hence the contour map of Fig. 4 holds for the cases which have the same B/α. For the parameters adopted here, $y = -2$ and 2 correspond to $\epsilon \simeq 15°$ and $\simeq 55°$, respectively, which explains the results in the lower panel of Fig. 3. In this case, resonant width in y is $\simeq 2$ for that in $\epsilon \simeq 20°$.

For other I and $B/\alpha(= \cos\epsilon_*)$, the libration range in y can change in principle. Resonance width depends on $\cos\epsilon_*$ and I as in Figures 5. Since α and B are dependent on a, different a corresponds to different $\cos\epsilon_*$. From these results and the results with other $\cos\epsilon_*$ and I, we found the resonance width changes approximately as $\propto I^{1/2}$ and weakly depends on $\cos\epsilon_*$. However, we will show the evolution trajectories on the $x - y$ plane do not change for other I and B/α, at least near a resonance.

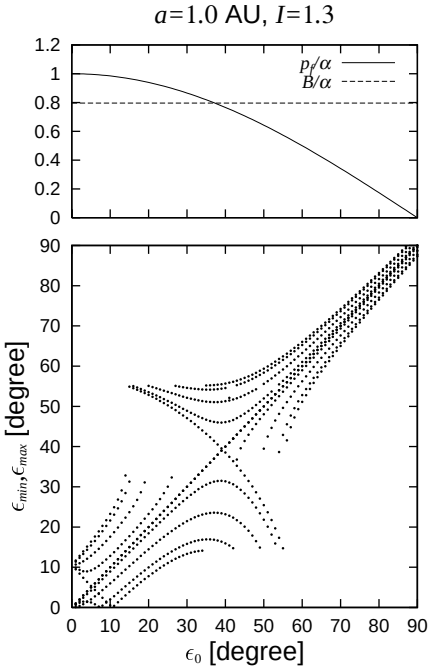

Figure 3: The lower panel is the minimum and maximum values of obliquity ϵ over 10^6 years calculation as a function of initial obliquity ϵ_0. p_f and B scaled by α are plotted in the upper panel.

4 Analytical calculation

We derive an analytical solution to Eq. (1) near a resonance. Near a resonance ($\alpha\cos\epsilon \simeq B$), Eqs. (2) – (4), (6) – (8), (13) and (14) lead to

$$\frac{d}{dt}x \simeq \alpha\beta y, \tag{16}$$

$$\frac{d}{dt}y = \frac{d}{dt}(\hat{\boldsymbol{s}}\cdot\hat{\boldsymbol{n}}) \simeq -\alpha\beta\sin x. \tag{17}$$

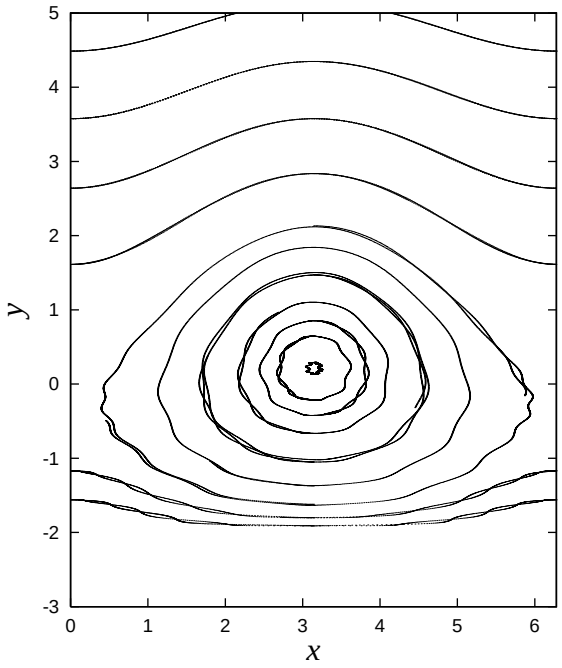

Figure 4: Trajectories on $x-y$ plane for the results with $\psi_0 - \Omega_0 = \pi$ in Fig. 3. Different trajectories correspond to runs with different $y_0(\epsilon_0)$.

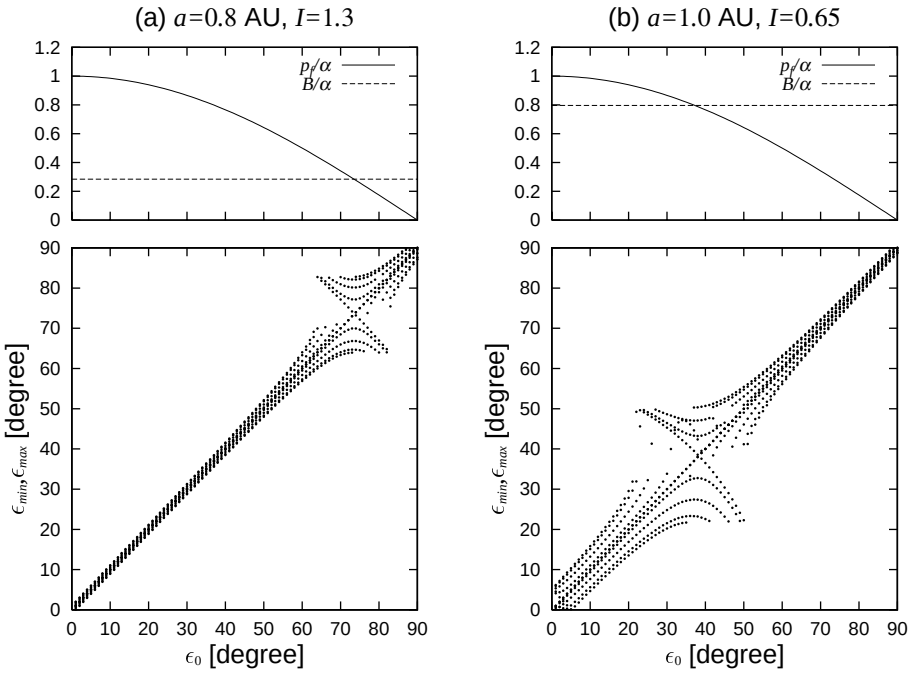

Figure 5: The same figures as Fig.2 expect for a or I. (a) $a = 0.8$ AU and $I = 1.3°$. (b) $a = 1.0$ AU and $I = 0.65°$.

In the right hand side of Eqs. (16) and (17), we retain the lowest order terms of I, assuming $I \ll 1$. With scaled variables

$$\tilde{t} = \alpha\beta t, \tag{18}$$

Eqs. (16) and (17) are reduced to

$$\frac{d}{d\tilde{t}}x \simeq y, \tag{19}$$

$$\frac{d}{d\tilde{t}}y \simeq \sin x, \tag{20}$$

which are independent of I and B/α. The equilibrium points are $y = 0$ and $\sin x = 0$ ($x = 0, \pi$). $x = 0$ is unstable against small displacements. $x = \pi$ is stable.

Let δx and δy be small displacements from the equilibrium point, $x = \pi$ and $y = 0$. Eqs. (19) and (20) gives

$$\frac{d}{d\tilde{t}}\delta x \simeq \delta y, \tag{21}$$

$$\frac{d}{d\tilde{t}}\delta y \simeq -\delta x. \tag{22}$$

The solution is

$$\delta x = C\cos(\tilde{t} + \gamma), \tag{23}$$

where C and γ are constants of integration which are determined by initial conditions ψ_0 and ϵ_0. Substituting Eq. (23) into Eq. (21), we have

$$\delta y = C\sin(\tilde{t} + \gamma). \tag{24}$$

Eqs. (23) and (24) represent librating motion centered at $x = \pi$ and $y = 0$ with libration period 2π in unit of $\tilde{t}$. The scaling factor $\alpha\sqrt{I\cos\epsilon_*\sin\epsilon_*}$ for $\tilde{t}$ appears to be angular velocity for the libration.

As mentioned in Sec. 3, if α, B and I are given, ϵ uniquely corresponds to some value y. Therefore Figure 4 explains the evolution of ϵ. If a starting point is on closed trajectory, x and y librate around the equilibrium point and ϵ exhibits large variation. Equations (19) and (20) have an integration as

$$H = \frac{1}{2}y^2 + \cos x, \tag{25}$$

where H is constant. Different values of H corresponds to different trajectories. In Fig. 4, we start with $\cos x = -1$. Thus, the trajectory with y_0 corresponds to the contour of $H = {y_0}^2/2 - 1$. Trajectories of libration correspond to $-1 \le \cos x \le 1$ at $y = 0$, which is equivalent to $-1 \le H \le 1$. Since $|y|$ takes a maximum value $= \sqrt{2(H+1)}$ at $\cos x = -1 (x = \pi)$ for each trajectory,

$$|y_{\max}| = 2. \tag{26}$$

In Fig. 6, these analytical estimates are compared with numerical results in Fig. 4, which agree with each other. Numerical results with other I and B/α also agree with the analytical estimates.

Therefore we derived the resonance width semi-analytically as

$$|\delta\cos\epsilon|_{\max} \simeq 2\sqrt{I\cos\epsilon_*\sin\epsilon_*}. \tag{27}$$

The dependence of $|\delta \cos\epsilon|_{\max}$ on ϵ_* and I as well as the magnitude in the above almost completely agrees with the numerical results. Ward et al. (1979) derived $|\delta\epsilon| \sim \sqrt{I/\tan\epsilon_*}$ at a resonance, through higher order expansion of Eq. (1), although the detailed derivation is not presented. Although his result does not have any dependence on ψ_0 and $\epsilon_0 - \epsilon_*$ and it includes uncertainty of a numerical factor, it is consistent with Eq. (27) in the limit of $\delta\epsilon \to 0$ expect for a numerical factor.

5 Conclusion and Discussion

We have investigated the evolution of obliquity through analytical arguments and numerical calculations. We re-analyzed the spin-orbit resonance in a more general form. We considered a system containing a host star, a hypothetical terrestrial planet, and a hypothetical giant planet, and calculated the evolution of obliquity ϵ of the terrestrial planet in wide ranges of parameters I, B, α, and initial conditions of ϵ and $\psi - \Omega$, where I is the orbital inclination, B is the frequency of the orbital variation, α is the precessional constant, ϵ is the obliquity, ψ is the precession angle, and Ω is the longitude of the ascending node.

We found the following results:

1. Evolution of obliquity is described by a contour map on the plane of $x = \psi - \Omega$ and $y = (\dot{\psi} - \dot{\Omega})/\alpha\sqrt{I(B/\alpha)\sqrt{1-(B/\alpha)^2}}$. Different contours correspond to different initial conditions of ϵ and $\psi - \Omega$. The contour map does not depend on I, B, and α.
2. In the librating region centered at a resonant point, $\cos\epsilon_* = B/\alpha$ and $\psi - \Omega = \pi$ $(x = \pi, y = 0)$, the obliquity has variations with large amplitudes (Fig. 3 and 4).
3. The width of libration region is $|\delta y|_{\max} = 2$, which reads as

$$|\delta \cos\epsilon|_{\max} \simeq 2\sqrt{I \cos\epsilon_* \sin\epsilon_*}. \tag{28}$$

The range of the obliquity variation near a resonance ϵ_* is

$$\cos^{-1}(\cos\epsilon_* + |\delta\cos\epsilon|_{\max}) \le \epsilon \le \cos^{-1}(\cos\epsilon_* - |\delta\cos\epsilon|_{\max}). \tag{29}$$

Note that the width of resonance region does not explicitly depend on the masses and semi-major axis of the terrestrial planet and the giant planet. In Figure 6, we plot this range as a function of a, in the case of $I = 1.3°$ and the other parameters given in section 4. If another giant planet is considered, the large variation regions are expressed by the superposition of spin-orbit resonances due to individual eigenfrequencies of orbital change of the terrestrial planet. If the resonant regions overlap, the obliquity variations could be chaotic.

Many extrasolar giant planets have been found around nearby solar-like stars. Substituting the masses and the semi-major axes of such planets, we can obtain the resonance regions where obliquity variations are large by the spin-orbit resonance if planetary ellipticities and spin rates are given. In a system with a giant planet with relatively large semi major axis, Earth-like planets (small rocky planets) may exist inside the orbits of the giant planet. For life to exist in such a Earth-like planet, the planet may need to have not only H_2O ocean but also orbit and obliquity with small variation to keep the climate stable. Assuming probable values of ellipticity and the spin rate, we may evaluate the probability of existence of such "habitable" planets in extrasolar systems. We will address this issue in next paper.

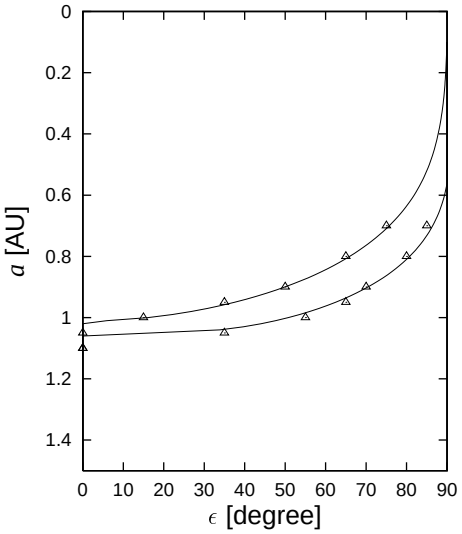

Figure 6: Resonance region in the case of $I = 1.3°$. The area between the two solid lines expresses a resonance region. Triangles show the numerical results. Solid lines express the analytical expression given by Eq. (29)

References

[1] Laskar, J. 1988. Secular evolution of the Solar System over 10 million years. *Astron. Astrophys.* **198**, 341–362.

[2] Laskar, J. 1990. The chaotic motion of the Solar System: a numerical estimate of the size of the chaotic zones. *Icarus* **88**, 266–291.

[3] Laskar, J., and P. Robutel 1993. The chaotic obliquity of the planets. *Nature* **361**, 608–612.

[4] Touma, J., and J. Wisdom 1993. The chaotic obliquity of Mars. *Science* **259**, 1294–1297.

[5] Ward, W.R. 1974. Climatic Variations on Mars 1. Astronomical theory of insolation. *J. Geophys .Res.* **79**, 3375–3386.

[6] Ward, W.R. 1979. Present obliquity oscillations of Mars: fourth-order accuracy in orbital e and I. *J. Geophys. Res.* **84**, 237–241.

[7] Ward, W.R. 1992. Long-term orbital and spin dynamics of Mars. In *Mars*, p.298–320. Univ. Arizona Press, Tucson.

[8] Ward, W.R., and D.J. Rudy 1991. Resonant obliquity of Mars? *Icarus* **94**, 160–164.